widths, it would be advantageous to use below-resonance operation, and this should be further investigated.

Further work is required to realize experimentally the splitting obtained in the analysis and to evaluate the practical bandwidth and frequency limitations of this approach. It is anticipated that the crossoverless miniature lumped-element circulator will be particularly important at the higher microwave frequencies since the close tolerances and critical processing steps required in the crossover approach are avoided.

Computer generated and measured results are in qualitative agreement verifying the validity of extending the assumptions of the Y theory to the crossoverless device. It should be noted, however, that the analysis assumes an ideal 100-percent coupling between the inductors without considering where the coupling is physically obtained.

REFERENCES

[1] R. H. Knerr, C. E. Barnes, and F. Bosch, "A compact broad-band thin-film lumped-element L-band circulator," *IEEE Trans. Microwave Theory Tech. (1970 Symposium Issue)*, vol. MTT-18, pp. 1100–1108, Dec. 1970.

[2] R. H. Knerr, "A 4-GHz lumped-element circulator," *IEEE Trans. Microwave Theory Tech.*, vol. MTT-21, pp. 150–151, Mar. 1973.

[3] ——, "A microwave circulator that is smaller than a quarter," *Bell Lab. Rec.*, vol. 51, pp. 78–84, Mar. 1973.

[4] M. Grace and F. R. Abrams, "Three-port ring circulators," *Proc. IRE*, vol. 48, pp. 1497–1498, Aug. 1960.

[5] S. D. Ewing, Jr., and J. A. Weiss, "Ring circulator theory, design and performance," *IEEE Trans. Microwave Theory Tech.*, vol. MTT-15, pp. 623–628, Nov. 1967.

[6] E. Pivit, "Zirkulatoren Aus Konzentrierten Schaltelementen," *Telefunken J.*, vol. 38, p. 206, 1965.

[7] H. J. Carlin, "Principles of gyrator networks," in *Proc. Symp. Modern Advances in Microwave Techniques* (Polytech. Inst. Brooklyn, Brooklyn, N. Y.), Nov. 1954.

[8] R. H. Knerr, "An improvement equivalent circuit for the thin-film lumped-element circulator," *IEEE Trans. Microwave Theory Tech.*, vol. MTT-20, pp. 446–452, July 1972.

[9] ——, "A proposed lumped-element switching circulator principle," *IEEE Trans. Microwave Theory Tech.*, vol. MTT-20, pp. 396–401, June 1972.

Slot-Line Transitions

JEFFREY B. KNORR, MEMBER, IEEE

***Abstract*—Coax–slot and microstrip–slot transitions are discussed. Experimental VSWR and impedance data are presented and compared with values computed using equivalent circuits for these transitions. Thick-film chip terminations are also investigated.**

I. INTRODUCTION

Coax–slot and microstrip–slot transitions have been employed by a number of investigators and some experimental VSWR data have been reported [1], [2]. Equivalent circuits for these transitions have also been proposed [3]. However, no comprehensive comparison of experimental and theoretical performance has yet been published. The purpose of this short paper is to present the results of a study which was undertaken to compare the theoretical and experimental performance of these transitions.

II. COAX–SLOT TRANSITION

The coax–slot transition is shown in Fig. 1. It is constructed by placing miniature coaxial cable against the conducting surface and perpendicular to the slot at one end of the substrate. The outer

Manuscript received July 16, 1973; revised December 20, 1973.
The author is with the Department of Electrical Engineering, Naval Postgraduate School, Monterey, Calif. 93940.

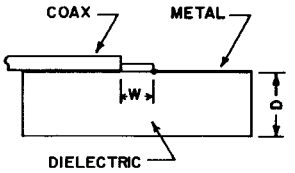

Fig. 1. Coax–slot transition.

conductor of the cable is electrically connected to one side of the slot with solder or epoxy and the center conductor is extended across the slot and bent down to meet the opposite edge where it is similarly secured. This is a rather easy transition to construct.

An approximate equivalent circuit for this geometrically complex transition has been obtained [3] through analysis of the simplified model shown in Fig. 2(a). The equivalent circuit is shown in Fig. 2(b) where

$$n = \frac{V(r)}{V_0} = \frac{\pi}{2} \mid k_c r H_1^{(1)}(k_c r) \mid \tag{1}$$

$$k_c = j\frac{2\pi}{\lambda'}\left(1 - \left\{\frac{\lambda'}{\lambda}\right\}^2\right)^{1/2}. \tag{2}$$

In these equations, $V(r)$ is the voltage at radius r, V_0 is the voltage directly across the slot, λ' is slot wavelength, and $H_1^{(1)}(k_c r)$ is a Hankel function. The coax–slot transition may be shunted by a short length of open-circuited slot line as well as by fringe capacitance at the open end of the slot. These effects are accounted for in the equivalent circuit by the lumped capacitance C. Typically, a millimeter of open-circuited 75-Ω slot line on a substrate with $\epsilon_r = 20$ has an input susceptance which is approximately equivalent to that of a 0.2-pF capacitor. L is the self-inductance of the semiloop of radius r.

Two coax–slot transitions were built and tested. The results were very similar for both and only one will be discussed in detail here. The transition was constructed with 50-Ω 0.141-in semirigid coaxial cable. This was coupled to a slot line etched from a 0.125-in-thick Custom Materials HI-K 707-20 ($\epsilon_r = 20$) substrate which was plated with 1 oz copper. Since the equivalent circuit predicts that the slot impedance will be transformed to a lower value, a slot impedance of about 75 Ω ($W/D = 0.55$) was selected. The slot was terminated at its other end with a 75-Ω thick-film chip resistor. The chip termination was obtained from EMC Technology, Inc., and consisted of a resistive film deposited on a 0.060- × 0.120- × 0.018-in alumina substrate. The chip was mounted upside down with epoxy thereby placing the resistive film directly across the slot. The termination has the same equivalent circuit as the transition, that of Fig. 2(b), with $n = 1$.

Experimental data for this transition were obtained using a microwave network analyzer. The reference plane was set at the transition and the data clearly indicated that the observed reflection coefficient was the vector sum of the reflection coefficients of the transition and the chip. The data were reduced accordingly using the theory of small reflections and the reflection coefficients of the two discontinuities were thus obtained. The method used did not account for losses due to radiation or attenuation in the slot, but these effects are believed to be very minor and any error is thus small.

The equivalent circuit of Fig. 2(b) was used to write equations for transition impedance and VSWR and these were then programmed. The values of slot impedance and slot wavelength required in the program were obtained from published curves [1]. Since there is no precise way to calculate L, C, or r, the program was used only for analysis in this study. The self-inductance L was measured using a TDR and found to be 0.61 nH so this value was used in all calculations. This left two undetermined parameters, C and r, and these were varied within reasonable limits to obtain agreement with experimental results.

The theoretical and experimental VSWR's of the transition are shown in Fig. 3. It can be seen that the experimental curve is in reasonable agreement with the theoretical curve for $C = 0$ pF. A radius $r = 0.1$ in was used in these calculations. This is about 50

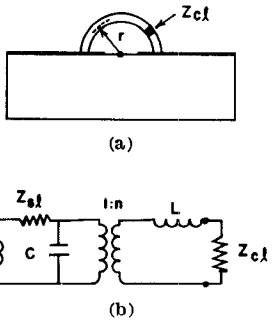

Fig. 2. (a) Simplified model of coax–slot transition. (b) Equivalent circuit of coax–slot transition.

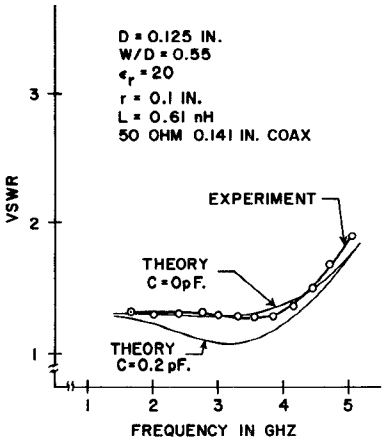

Fig. 3. VSWR versus frequency for 0.141-in coax–slot transition.

percent greater than the actual height of the center conductor above the slot. Theoretical curves computed using smaller values of radius were not in agreement with measurements.

It is possible to suggest two reasons for the need to use a larger than actual radius in making theoretical calculations. First, the actual geometry differs from that of the simplified model of Fig. 2(a). It is difficult to make the inner conductor of the coax follow a circular path, and further, it must emanate from the coaxial cable on one side of the slot and thus cannot form a full semiloop. Second, the Hankel function approximation to the electric field on the air side of the metal was used in deriving the equivalent circuit and this becomes inaccurate in the immediate neighborhood of the slot. In practice, the transition must be constructed with the coax directly across the slot if the transition is to have a broad bandwidth. The penalty for not placing the coax directly across the slot is a rapidly increasing high VSWR at the high-frequency end of the operating range. This is caused by a decreasing induced voltage as the fields become more tightly bound to the slot with increasing frequency. Thus, in the equivalent circuit, the use of a radius equal to one-half the cable diameter does not result in a proper transformer turns ratio.

These conclusions were confirmed in experiments with a second identical slot line having a 50-Ω 0.085-in semirigid coax transition. The closer proximity of the center conductor to the slot and its somewhat lower self-inductance resulted in a lower VSWR. It was again found that use of an effective radius about 50 percent greater than the actual radius produced the best correlation between theory and experiment.

A Smith chart plot of the theoretical and experimental impedance of the 0.141-in coax transition is shown in Fig. 4. Theoretical parameters are the same as those used for the calculations of Fig. 3. The frequency range for each of the curves is 1.65–5.05 GHz. The correlation between theory ($C = 0$ pF) and experiment is quite good up to about 4 GHz. At this point, the experimental data indicate a rapidly increasing component of inductive reactance which is not predicted by the equivalent circuit. This same phenomenon was observed again in experiments with the 0.085-in transition mentioned earlier.

The VSWR of the 75-Ω chip termination is shown in Fig. 5. Below 4 GHz, it is less than 1.15. Above 4 GHz, the VSWR begins to increase due primarily to the self-inductance. For reference, the slot impedance varies from about 73 to 78 Ω over the frequency range shown.

III. MICROSTRIP–SLOT TRANSITION

The microstrip–slot transition is shown in Fig. 6(a). The slot, which is etched on one side of the substrate, is crossed at a right angle by a microstrip conductor on the opposite side. The microstrip extends about one-quarter of a wavelength beyond the slot and similarly, the slot extends about one-quarter of a wavelength beyond the microstrip.

An equivalent circuit for the microstrip–slot transition is given in [3]. This equivalent circuit is shown in Fig. 6(b) where

Z_{sl} slot impedance;
θ_{sl} electrical length of slot stub;
X_{sl} equivalent reactance of shorted slot;
Z_{ms} microstrip impedance;
θ_{ms} electrical length of microstrip stub;
C_{oc} equivalent capacitance of open microstrip;

and

$$n = \cos 2\pi \frac{D}{\lambda} u - \cot q_0' \sin 2\pi \frac{D}{\lambda} u \tag{3}$$

$$q_0' = 2\pi \frac{D}{\lambda} u + \tan^{-1}\left(\frac{u}{v}\right) \tag{4}$$

$$u = \left[\epsilon_r - \left(\frac{\lambda}{\lambda'}\right)^2\right]^{1/2} \tag{5}$$

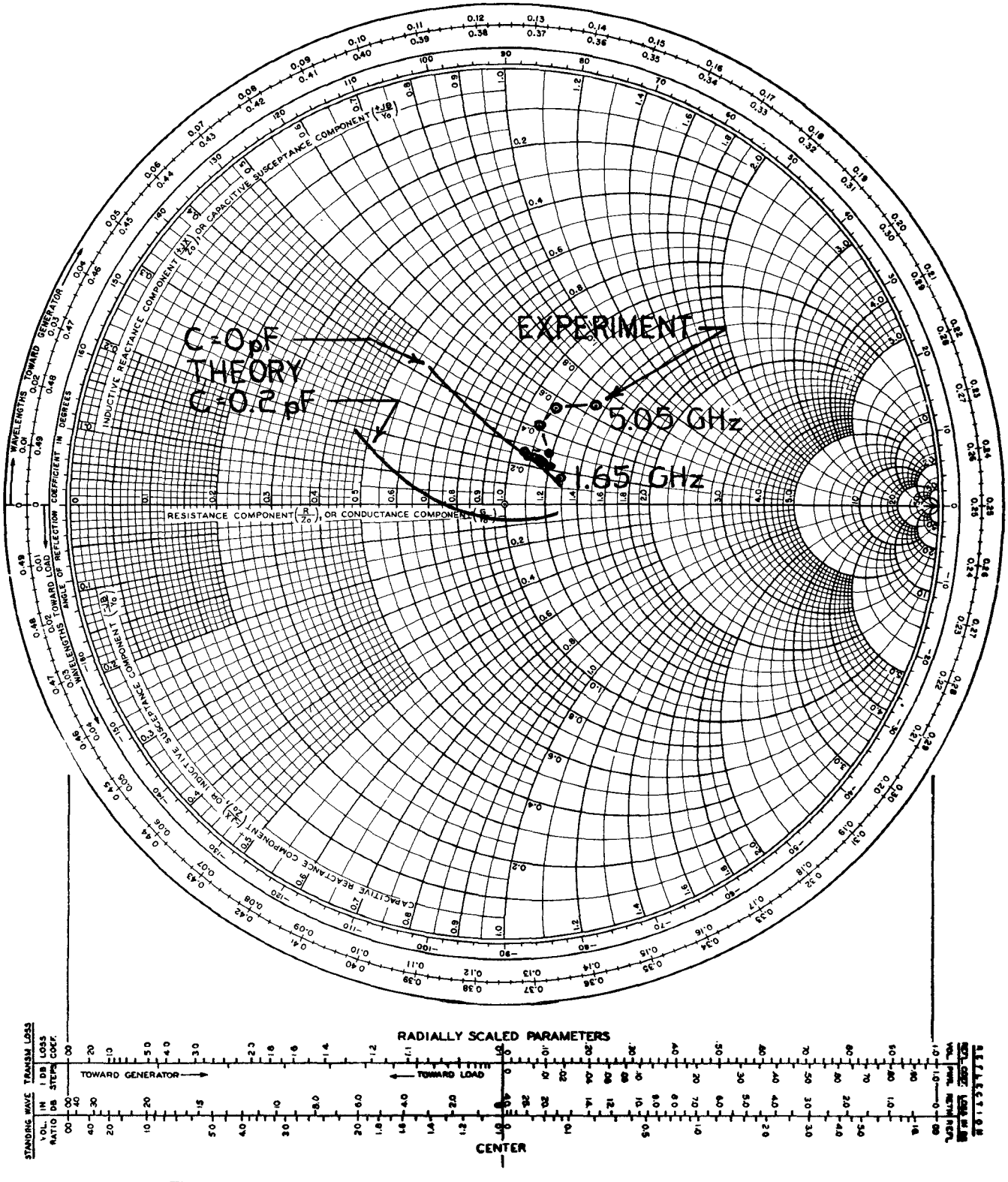

Fig. 4. Smith chart plot of impedance versus frequency for 0.141-in coax–slot transition.

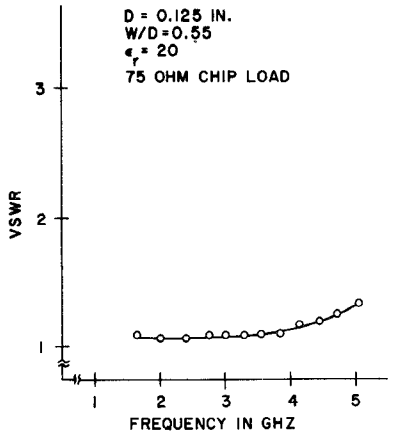

Fig. 5. VSWR versus frequency for 75-Ω chip termination.

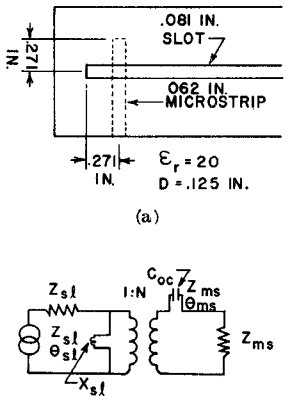

Fig. 6. (a) Microstrip–slot transition. (b) Equivalent circuit of microstrip–slot transition.

$$v = \left[\left(\frac{\lambda}{\lambda'}\right)^2 - 1\right]^{1/2}. \tag{6}$$

From an inspection of the equivalent circuit it is clear that a perfect match can be achieved at a given frequency by making

$$Z_{sl} = \frac{Z_{ms}}{n^2} \tag{7a}$$

$$B_{sl}{}^{in} = 0 \tag{7b}$$

$$X_{ms}{}^{in} = 0 \tag{7c}$$

where $B_{sl}{}^{in}$ is the susceptance looking into the shorted slot stub and $X_{ms}{}^{in}$ is the reactance looking into the open-circuited microstrip stub.

A computer program based upon the equivalent circuit of Fig. 6(b) was written for the purpose of analyzing and designing microstrip–slot transitions. The curves of [1] were again used to obtain the necessary values of Z_{sl} and λ'/λ. The equivalent inductive reactance of a shorted slot has been measured experimentally in our laboratory and slot end effect was accounted for in this manner [4]. The equivalent capacitance of the microstrip open circuit was determined from [5].

The material from which the microstrip transition was constructed was 0.125-in-thick Custom HiK 707-20 ($\epsilon_r = 20$). The microstrip impedance was chosen as 50 Ω and the computer program was used to optimize the transition for a VSWR of one at 3 GHz. The procedure used was to choose a value of $(W/D)_{sl}$ giving a slot impedance somewhat greater than Z_{ms}. The stub lengths were chosen for resonance at 3 GHz. The computer program was then used to obtain the (real) impedance seen by the slot at the design frequency of 3 GHz. The slot stub length was readjusted and the process was repeated until the design was optimized. The impedance and VSWR of the transition were then computed.

Convergence by the process described is quite rapid. In our computations, an initial value of $Z_{sl} = 70$ Ω was chosen. The computer program indicated a second iteration using $Z_{sl} = 80$ Ω at 3 GHz and this resulted in a VSWR of about 1.01 at 3 GHz. This was considered close enough to optimum and a transition was fabricated.

After the transition was fabricated, dimensions were checked and found to be close to the intended design values. Actual dimensions are shown in Fig. 6(a). In the design, it was assumed that stub length should be measured from line center.

The nominal 80-Ω slot was terminated with a 75-Ω chip resistor and VSWR measurements were made looking into the microstrip–slot transition. A network analyzer was used as before. The experimental data points which were obtained are plotted in Fig. 7. In those regions where transition VSWR is high, any reflection from the chip termination is effectively masked and thus no attempt was made to separate reflections through data reduction. In the 2–4-GHz range, some ripple due to the reflection from the termination can be seen, however.

The theoretical curve in Fig. 7 was computed using the actual dimensions of the fabricated transition. The flat bottom of the curve in the neighborhood of 3 GHz resulted because the two stubs were resonant at slightly different frequencies. We also note that the experimental data show the center frequency of this transition is somewhat greater than the 3-GHz design frequency. This indicates that the effective stub lengths were somewhat less than the distance measured from line center to stub end.

In view of the discrepancy between theory and experiment revealed by Fig. 7, a second theoretical computation was made. In this case, each stub length was measured from the edge of the opposite line. The result of this computation is displayed in Fig. 8 along with

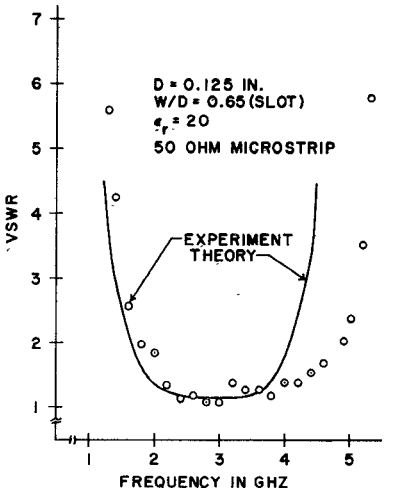

Fig. 7. VSWR versus frequency for microstrip–slot transition. Stub lengths measured from line center.

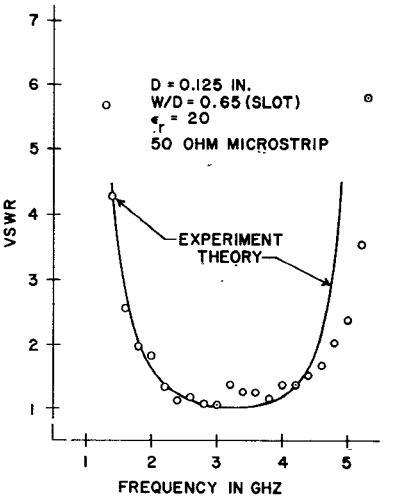

Fig. 8. VSWR versus frequency for microstrip–slot transition. Stub lengths measured from line edge.

the experimental data points. It is evident that this choice of stub length results in very good agreement between theoretical and experimental VSWR.

The theoretical and experimental values of impedance for the microstrip transition are shown in Fig. 9. The theoretical curve was computed for the same conditions as the calculations of Fig. 8 with stub length measured from the edge of the opposite line. As pointed out earlier, the experimental data contain components due to both the transition and the chip termination. The contribution from the chip is small, however, and thus a valid comparison of theory and experiment can be made. The data reveal that while the experimental reflection coefficient has approximately the same magnitude as predicted theoretically there is a considerable phase error. This error is about 50° at the frequency extremes of 1.5 and 5 GHz shown in Fig. 9.

IV. RADIATION EFFECTS

During the course of this study, it was discovered that radiation took place in the vicinity of coax–slot transitions and chip terminations. This was observable as a very minor change in reflected power (VSWR) when a reflecting object was moved around the end of the substrate. The movement of a hand, for example, could create this effect at a distance of 1–2 ft. It is believed that this effect was due to the open-ended slot line. The fact that no radiation was observed during preliminary investigation of a coax–slot transition backed by a shorted stub tends to substantiate this theory. The microstrip–slot transition did not radiate.

V. CONCLUSIONS

Coax–slot and microstrip–slot transitions have been investigated and their experimental performance has been compared with theory. The equivalent circuits of these transitions are of the correct form and give a reasonably accurate prediction of the VSWR. There is some discrepancy, however, between the impedance predicted by these equivalent circuits and that observed experimentally.

Practically, the performance of the coax–slot transition is best when the center conductor of the coax is as close as possible to the slot. Performance thus improves with decreasing diameter of the coax. The limiting factor with these transitions appears to be the self-inductance which results in a VSWR which increases at the high-frequency end of the operating range.

The microstrip to slot transition has the advantage that it may be fabricated using only an etching process and is thus easily reproducible. A VSWR < 1.5 was obtained over a 60-percent fractional bandwidth. Since all the electrical properties of this transition scale with wavelength it is an attractive choice for the higher frequencies.

Secondarily, this study has shown that an open-ended slot line is suspect as a minor source of radiation and that thick-film chip

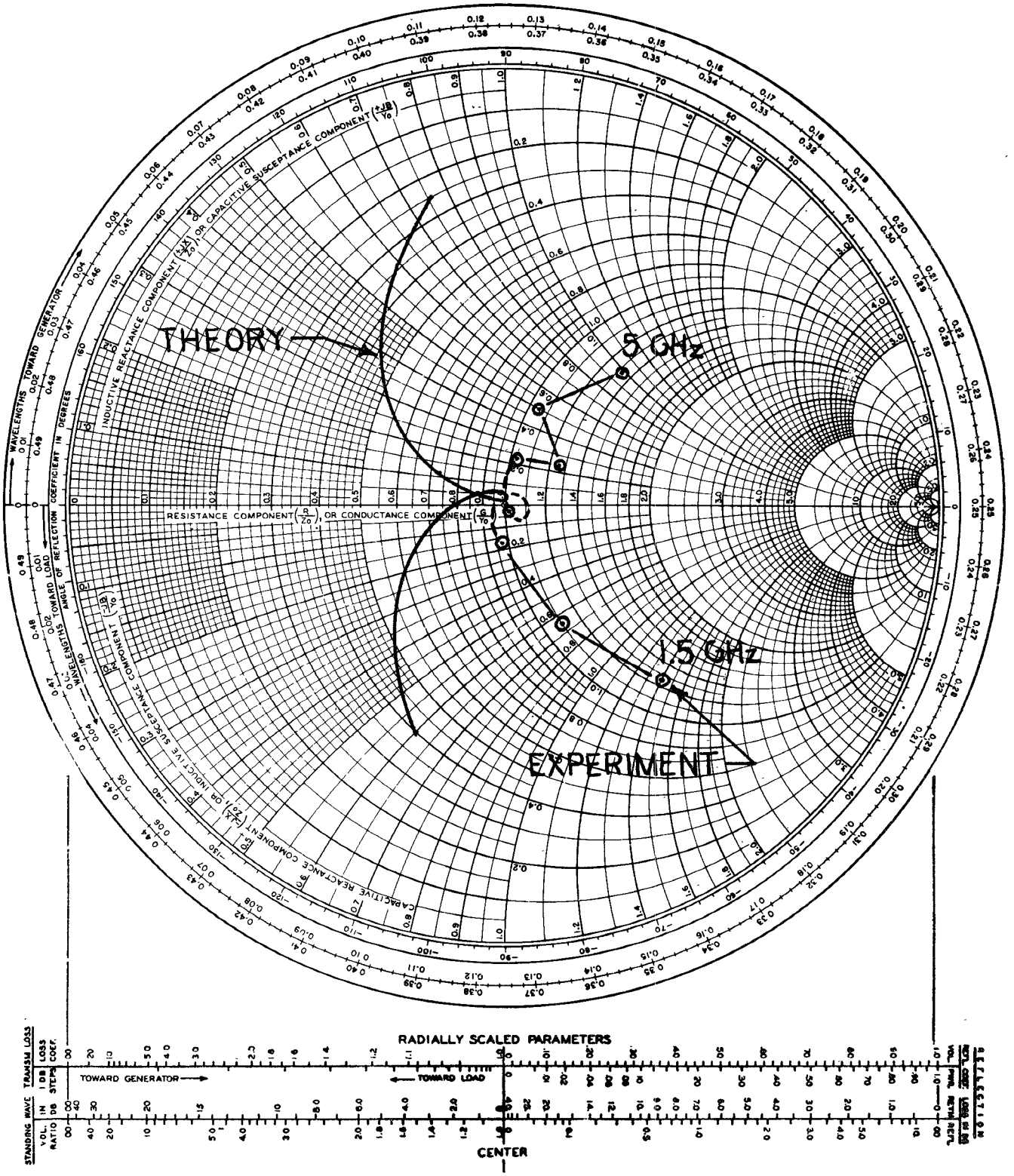

Fig. 9. Smith chart plot of impedance versus frequency for microstrip–slot transition.

resistors provide reasonably good terminations at least to 5 GHz. The performance of the chip termination further documents the case for placing any transducer of this type directly across the slot.

REFERENCES

[1] E. A. Mariani, C. P. Heinzman, J. P. Agrios, and S. B. Cohn, "Slot line characteristics," *IEEE Trans. Microwave Theory Tech. (1969 Symposium Issue)*, vol. MTT-17, pp. 1091–1096, Dec. 1969.

[2] G. H. Robinson and J. L. Allen, "Slot line application to miniature ferrite devices," *IEEE Trans. Microwave Theory Tech. (1969 Symposium Issue)*, vol. MTT-17, pp. 1097–1101, Dec. 1969.

[3] D. Chambers, S. B. Cohn, E. G. Cristol, and F. Young, "Microwave active network synthesis," Stanford Res. Inst., Menlo Park, Calif., Semiannual Rep., Contract DAAB07-C-0044, SRI Project 8254, June 1970.

[4] J. B. Knorr and J. Saenz, "End effect in a shorted slot," *IEEE Trans Microwave Theory Tech.*, vol. MTT-21, pp. 579–580, Sept. 1973.

[5] P. Silvester and P. Benedek, "Equivalent capacitances of microstrip open circuits," *IEEE Trans. Microwave Theory Tech.*, vol. MTT-20, pp. 511–516, Aug. 1972.

Analytic Model for Varactor-Tuned Waveguide Gunn Oscillators

A. S. TEMPLIN AND R. L. GUNSHOR, SENIOR MEMBER, IEEE

***Abstract*—An analytic model for electronic tuning of an X-band waveguide transferred-electron oscillator is presented. The oscillator is electronically tunable by a varactor, and mechanically tunable by movement of a short circuit. The model is used to predict oscillation frequency, maximum electronic tuning range, and electronic tuning versus varactor bias voltage. Two different methods, the "zero reactance theory" and the Slater perturbation theory, are used to calculate the electronic tuning. The results of these calculations are compared to experimental results for two different oscillator configurations.**

INTRODUCTION

The objective of this short paper is a theoretical prediction of both the mechanical and electronic tuning characteristics for a varactor-tuned oscillator using a transferred-electron device operated CW and mounted in full-height X-band waveguides. Wide electronic tuning ranges can be obtained using coaxial structures [1] or reduced-height waveguides [2]. When low FM noise is desired, higher Q structures involving waveguide cavities with their associated smaller tuning ranges are useful.

The input data for the calculations reported consist of the dimensions of the waveguide and mounting posts together with the usually specified varactor and Gunn diode parameters, including device package parameters for both. In this short paper we present an analytical model, and compare calculations based on this model using two different theories, with experimental data. Several Gunn diodes and varactors have been used in two oscillator configurations with typical results reported here.

ANALYTIC MODEL

The basis for the calculations in this paper is an extension of a previously reported model used to predict the mechanical tuning of a waveguide-mounted Gunn device, with and without a coupling iris [3]. In this equivalent circuit representation the mounting post is represented by the Marcuvitz theory for a finite diameter inductive post [4], while the capacitive gap in which the device is placed is included using the theory of Eisenhart and Khan [5].

Manuscript received July 18, 1973; revised December 17, 1973. This work was supported by the National Science Foundation under Grant GK11958 and by the Purdue University NSF-MRL Program.

A. S. Templin was with the School of Electrical Engineering, Purdue University, W. Lafayette, Ind. 47907. He is now with the Systems Group, TRW Corporation, Redondo Beach, Calif. 90278.

R. L. Gunshor is with the School of Electrical Engineering, Purdue University, W. Lafayette, Ind. 47907.

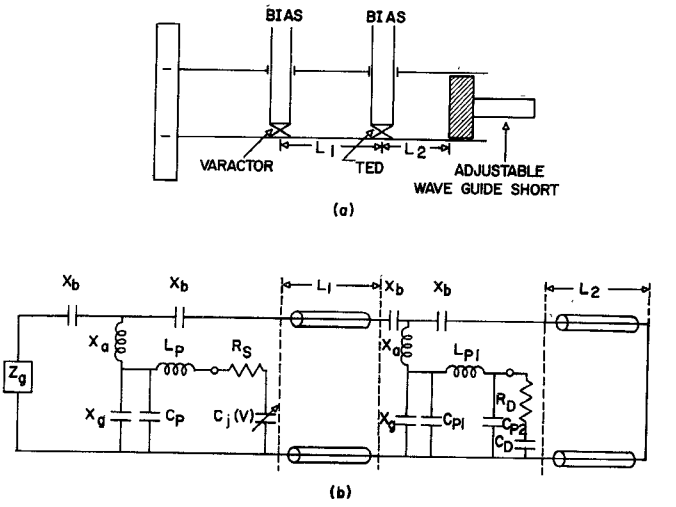

Fig. 1. (a) Oscillator configuration for case 1; case 2 is obtained by interchanging the varactor and Gunn device. The waveguide inside dimensions are 0.900 × 0.400 in; the two posts have a diameter of 0.120 in. (b) The equivalent circuit. X_a and X_b represent the post(s) as given by the Marcuvitz theory; X_g is the gap reactance from Eisenhart and Khan [5]. C_p and L_p are varactor package parameters; R_s is the varactor series resistance; and C_j is the junction capacitance. C_{p1}, C_{p2}, and L_{p1} are Gunn device package parameters; C_D and R_D are to represent the GaAs chip. The Gunn devices for the data shown here are Microwave Associates MA49156; the varactors are MA45103. L_1 and L_2 are lengths of waveguide with characteristic impedance $Z_g(\omega)$.

In this paper we add an additional mounting post for the varactor, together with the varactor and associated package parameters, to the previously described model. The resulting equivalent circuit is shown in Fig. 1. The varactor and Gunn diode parameters are those specified by the commercial manufacturers.

Computations are performed with a digital computer using two different methods to determine the change in frequency due to a change in varactor bias.

In the first method, which we call the "zero reactance theory" [3]–[7] the center frequency of the Gunn oscillator is calculated using a search for frequencies such that the conditions corresponding to stable circuit-controlled oscillations are met, namely,

$$X_T(\omega) = X_D(\omega) + X_L(\omega) = 0 \tag{1}$$

$$\partial X_T/\partial\omega > 0 \tag{2}$$

where $X_D(\omega)$ is the reactance of the Gunn device at the oscillation frequency and $X_L(\omega)$ is the load reactance seen by the Gunn device.

Electronic tuning is calculated as a shift in oscillation frequency as the varactor dc bias is varied. This, of course, necessitates expressing the varactor junction capacitance as a function of bias voltage, such that the change in load reactance seen by the Gunn device may be calculated for a change in varactor bias voltage.

One of several differences between these calculations and those previously reported [7] is the retention of the varactor series resistance R_s. This loss element affects the range of electronic tuning, and is especially significant for the calculation of electronic tuning using our second method which is based on Slater perturbation theory [8].

SLATER PERTURBATION THEORY

The Slater perturbation theory is often applied in techniques for determining electromagnetic field configurations in resonant structures by introducing a perturbing volume and measuring the resultant shift in resonant frequency. In our second method for calculating electric tuning, the varactor may be thought of as a perturbing volume within the larger oscillator resonator. It can then be shown that (see Appendix)

$$\frac{\delta f}{f} \simeq \frac{Q_v\delta P_v + P_v\delta Q_v}{(P_0 + P_v)Q_L} \tag{3}$$

where Q_v is the varactor Q given by

$$Q_v = 1/\omega R_s C_j. \tag{5}$$